Effect of Alkali Concentration on the Nanofibrillation Efficiency of Cellulose by Mechanical Grinding

Jiwook Yang , Kyojung Hwang , Jaejung Lee , Sang-Jin Chun , Jimin Lee, and Jaegyoung Gwon , *

Efficient production of cellulose nanofibers (CNFs) from wood pulp remains a challenge for industrial applications, requiring optimized pretreatment and processing strategies. In this study, hardwood kraft pulp (Hw-BKP) was pretreated with NaOH solutions (5 to 20 wt%) and subsequently processed using a large-scale wet grinder. The effects of pretreatment concentration and grinding on nanofibrillation efficiency were evaluated through compositional, structural, and optical analyses. Alkali pretreatment promoted hemicellulose removal and crystalline transformation, while mechanical grinding facilitated progressive microfibrillation. Notably, pretreatment at concentrations above 15 wt% significantly enhanced nanofibrillation efficiency, highlighting the importance of crystalline transformation in addition to hemicellulose removal. These findings provide practical insights for optimizing CNF production processes and advancing their industrial-scale commercialization.

DOI: 10.15376/biores.21.1.288-304

Keywords: NaOH pretreatment; Mercerization; Grinder; Cellulose nanofibers; Hardwood bleached kraft pulp

Contact information: Forest Products and Industry Department, National Institute of Forest Science, 57 Hoegi-ro, Dongdaemun-gu, Seoul 02455, South Korea; *Corresponding author: gwonjg@korea.kr

INTRODUCTION

Cellulose nanofibers (CNFs) exhibit distinctive features such as high specific surface area and aspect ratio, low density, tunable surface nature, and excellent mechanical strength. Owing to their naturally derived composition, excellent biocompatibility, and multifunctional nanoscale characteristics, CNFs are emerging as key materials in biomedical engineering, energy storage systems, and environmental remediation (Meyabadi et al. 2014; Ganesan and Rengarajan 2022; Hajikhani and Lin 2022; Hiwrale et al. 2023). Nanofibers can be manufactured by bottom-up approaches such as self-assembly, electrospinning, and phase separation, or by top-down methods involving chemical and mechanical treatments such as grinding and high-pressure homogenization. It's also possible to make nanofibers biologically, using microbes or enzymes. Among these, the top-down approach has the advantage due to its simple process and high productivity, making it suitable for large-scale production. Wood-derived pulp, in particular, has drawn continued attention as raw material of nanofibers because it's not only plentiful but also offers high purity (Barhoum et al. 2019; Carter et al. 2021; Djafari Petroudy et al. 2021; Ganesan and Rengarajan 2022; Ke et al. 2022). Cellulose is a linear polymer composed of β-1,4-glycosidic linkages, naturally synthesized in plants, microorganisms, and algae. It is the most abundant natural polymer on Earth, with an annual global production of approximately 1.5 trillion tons. Cellulose-based nanofibers are actively studied in a wide

range of applications due to their outstanding properties such as high mechanical strength, transparency, flexibility, and biodegradability (Kassie *et al.* 2024).

Representative top-down mechanical methods for producing nanofibers from cellulose include high-pressure homogenization, microfluidization, and ultrafine grinding. Each method differs in energy consumption, productivity, and processing efficiency. High-pressure homogenizers generate strong shear forces, enabling the production of highly uniform CNFs, but they consume significant energy (1.1 to 8.8 kWh/kg), especially with repeated passes, and often require costly maintenance. Microfluidizers consume 0.06 to 0.18 kWh/kg per cycle depending on the pressure, with total energy use averaging around 2.55 kWh/kg for full processing. They can produce high-quality, uniform nanofibers and offer advantages in particle size control. However, they also suffer from drawbacks such as pressure-dependent energy spikes, slower throughput, and clogging issues. In contrast, ultrafine grinders are valued for their lower energy demands (1.3 to 3.1 kWh/kg) and suitability for continuous processing. Although they may yield fibers with less uniformity, they are often preferred in large-scale operations due to their economic and operational advantages (Spence *et al.* 2011; Nechyporchuk *et al.* 2016; Djafari Petroudy *et al.* 2021; Pradhan *et al.* 2022; Yao *et al.* 2023; Jose *et al.* 2025).

To enhance the production and nanofibrillation efficiency of cellulose nanofibers through the mechanical treatments, various chemical pretreatments have been introduced prior to the mechanical disintegration of the pulp (micro sized cellulose). Chemical pretreatment facilitates the disintegration of cellulose by removing hemicellulose and loosening the crystalline structure, thereby improving fibrillation efficiency. Typical approaches include TEMPO-mediated oxidation, alkali treatment, and enzymatic hydrolysis. Among them, alkali treatment with NaOH has long been employed in cellulose chemistry due to its low cost and ability to remove hemicellulose, which adheres to elementary cellulose fibrils. Hence, the alkali treatment, when combined with mechanical processing, represents a cost-effective strategy for producing cellulose nanofibers. Alkali treatment of sufficiently high concentration removes hemicellulose and lignin from the wood fiber and rearranges hydrogen bonds between cellulose molecules.

The interaction between alkali and cellulose has been extensively studied, revealing that alkali treatment induces a transformation from the native cellulose I to the thermodynamically more stable cellulose II (Yue et al. 2013; Wang et al. 2014). The resulting cellulose II has improved thermal stability and reactivity (Yue et al. 2013; Wang et al. 2014). The structural conversion occurs as sodium hydroxide hydrates penetrate and swell the cellulose fibers, forming intermediate alkali-cellulose complexes. During this process, the molecular arrangement shifts from a parallel chain configuration (cellulose I) to an antiparallel configuration (cellulose II) through diffusion-driven reorganization within the crystalline lattice (Dinand et al. 2002; Banvillet et al. 2021). When cellulose is exposed to concentrated alkali solutions, its crystalline regions swell and subsequently rearrange upon washing, leading to the formation of a new polymorphic structure known as cellulose II (mercerization) (Dinand et al. 2002). In film applications, this CNF produced via mercerization exhibited the potential to tailor film properties through the formation of a continuous network and controlled crystalline structures (Banvillet et al. 2021). Furthermore, to enhance the nanofibrillation efficiency of micro-sized cellulose, it has been reported that incorporating enzyme pretreatment allows high-concentration alkali-treated cellulose to improve enzyme accessibility to the cellulose surface, consequently enhancing both the hydrolysis reaction rate and yield (Kuo and Lee 2009; Kobayashi et al. 2012; Sibila et al. 2016; Ling et al. 2017a). Still, most of the existing literature has primarily

addressed improvements in fiber characteristics such as crystallinity, thermal properties, or hydrophilicity. Far fewer studies have looked into how varying alkali concentrations interact with mechanical grinding, or how these factors can be optimized together to improve nanofibers' quality, scalability, and production efficiency (Jonoobi *et al.* 2015; Nechyporchuk *et al.* 2016; Cao *et al.* 2022; Jose *et al.* 2025).

In this study, hardwood kraft pulp was subjected to alkali pretreatment using aqueous NaOH solutions at concentrations of 5, 10, 15, and 20 wt%. The pretreated pulp was then mechanically processed using a large-scale wet grinder (MKZA15-40J) to produce CNFs. The manufactured nanofibers were evaluated for their physicochemical characteristics to evaluate how different alkali pretreatment concentrations and mechanical treatment conditions affect nanofibrillation efficiency. Based on these results, the study aimed to support the development of optimized processes for large-scale CNF production and to provide fundamental data for the design of industrial-scale processes and future commercialization of CNFs.

EXPERIMENTAL

Materials

Sheet-type hardwood bleached kraft pulp (Hw-BKP), consisting of mixed hardwood species (oak and acacia), was provided by Moorim Paper Co., Ltd. (Ulsan, South Korea). NaOH (>98%, Daejung, Siheung, Korea) was used for alkaline pretreatment.

Pretreatment and Disintegration of Hardwood Kraft Pulp Hw-BKP

Alkali pretreatment

The Hw-BKP was shredded into approximately 2 × 2 cm pieces and dried before use. Alkali pretreatment was conducted at room temperature using NaOH aqueous solutions with concentrations of 5, 10, 15, and 20 wt%, following a modified TAPPI method (T203 cm-99). Each sample was treated for 1 hour and then thoroughly washed with tap water using a 200-mesh sieve until neutral pH was reached.

Mechanical treatment

The pretreated pulp was dispersed in water to prepare a 1 wt% suspension. This suspension was processed using a grinder (colloid mill, MKZA15-40J, Masuko Sangyo Co. Ltd., Kawaguchi, Japan) with a throughput capacity of approximately 200 to 1000 kg/h and a disk diameter of 360 mm. The clearance was first adjusted to a 50 µm disc gap without any sample and rotating the discs at 1,740 rpm. When the sample passed through the discs, the clearance was set to –200 µm. Prior to reaching the target clearance, the sample that had passed through the grinder was collected and reprocessed to ensure uniform treatment. The mechanical grinding speed was maintained at *ca.* 6 kg/min, providing consistent nanofibrillation efficiency across the number of passes. The total suspension processed, including cellulose, was approximately 90 kg. Nanofibrillation was performed in multiple passes, up to 80 passes, with evaluations at 20-pass intervals.

Analysis of the Physicochemical Properties of the Cellulose Nanofibers

X-ray diffraction (XRD) analysis

Sheets were prepared from Hw-BKP treated with various concentrations of alkali and grinder treatment, and then analyzed using an X-ray diffractometer (DMAX-2500,

Rigaku, Tokyo, Japan). The diffraction patterns were measured in the 2θ range of 10 to 40 degrees, using Cu K α radiation (40 kV, 200 mA) at a scanning rate of 2°/min.

Scanning electron microscopy (SEM) analysis

The morphological characteristics of alkali-pretreated and grinder-treated Hw-BKP were analyzed using field-emission scanning electron microscopy (FE-SEM). To prepare the sample, Hw-BKP nanofiber (CNF) suspension was diluted to 0.002 wt% and dispersed for 30 seconds using an ultrasonic homogenizer (VCX130, Sonics & Materials, Newtown, CT, USA). The suspension was then vacuum-filtered through a 0.1 µm PTFE membrane filter (Advantec, Japan) and solvent-exchanged three times with tert-butyl alcohol. The sample was stored at -60 °C for 24 h and then freeze-dried for 72 h using a freeze dryer (LP-03, Ilshin biobase, Dongducheon, Korea). The dried specimens were coated with a 2 nm layer of iridium (Ir) using a sputter coater (EM ACE600, Leica, Wetzlar, Germany) and observed under an ultra-high-resolution scanning electron microscope (UH-SEM, S-4800, Hitachi, Tokyo, Japan) operated at an accelerating voltage of 5 kV.

Fiber morphology evaluation

The manufactured Hw-BKP nanofibers were evaluated for their dimensional properties using image analysis software ImageJ (National Institutes of Health, Bethesda, MD, USA) based on SEM images. The average fiber diameter was calculated from measurements of approximately 300 individual fibers. For fiber length, coarseness, and fines measurement, alkali-pretreated Hw-BKP suspensions were prepared at a solid content of 0.1 g, and the measurements were conducted using an L&W Fiber Tester Plus (ABB AB/Lorentzen & Wettre, Kista, Sweden).

Chemical composition analysis

The compositional changes of Hw-BKP resulting from alkali pretreatment and mechanical processing were evaluated by sugar analysis. For this analysis, 0.2 g of dried sample was mixed with 3 mL of 72% (w/w) sulfuric acid (Daejung Chemicals, Siheung, Korea) and stirred for 2 h. The hydrolyzed solution was then diluted to 4% and subjected to a second-stage hydrolysis in an autoclave at 121 °C for 1 h. The completely hydrolyzed sample was filtered through a 0.45 μ m membrane syringe filter (Whatman, Cytiva, Maidstone, UK) and analyzed using high-pressure liquid chromatography (HPLC) (1290 Infinity II, Agilent Technologies, Santa Clara, CA, USA). An Aminex HPX-87H column (300 × 7.8 mm, Bio-Rad Laboratories Inc., Hercules, CA, USA) and a refractive index detector (1290 Infinity LC, Agilent Technologies, Santa Clara, CA, USA) were used. The column temperature was maintained at 40 °C, and 0.01 N sulfuric acid was used as the mobile phase at a flow rate of 0.6 mL/min to evaluate changes in the chemical composition.

Optical properties

To characterize the optical properties of CNF, the alkali- and grinder-treated Hw-BKP suspensions were prepared at a concentration of 0.04 wt% and homogenized using a sonicator (VCX 130, Sonics & Materials, Newtown, CT, USA) at 300 W for 3 min. Subsequently, the suspensions were centrifuged at 1,000 g for 15 min using a centrifuge (Supra R22, Hanil Scientific Inc., Gimpo, Korea) to separate the supernatant containing nanofibers. The separated Hw-BKP nanofibers were characterized by measuring absorbance in the wavelength range of 200 to 600 nm using a UV/VIS spectrophotometer (Optizen POP, Mecasys Co., Ltd., Daejeon, Korea), and turbidity was determined using a

turbidity meter (TL2360, Hach Company, Loveland, CO, USA). Morphological analysis of the alkali-treated pulps was performed using an optical microscope (Axio Imager A1, Carl Zeiss Microscopy GmbH, Germany). For sample preparation, 1 wt% cellulose suspension was dropped (200 µL) onto a glass slide together with methylene blue solution (200 µL) for staining. The mixture was gently spread over the slide using a glass rod to achieve uniform dispersion. Subsequently, excess moisture and dye were carefully removed using a lint-free wipe (WypAll, Kimberly-Clark, USA), and the remaining fibers on the slide were observed under the microscope.

RESULTS AND DISCUSSION

Effect of Alkali Pretreatment Concentration on the Properties of Hw-BKP

Figure 1(a) presents the variation in sugar yield of Hw-BKP according to the alkali pretreatment concentration.

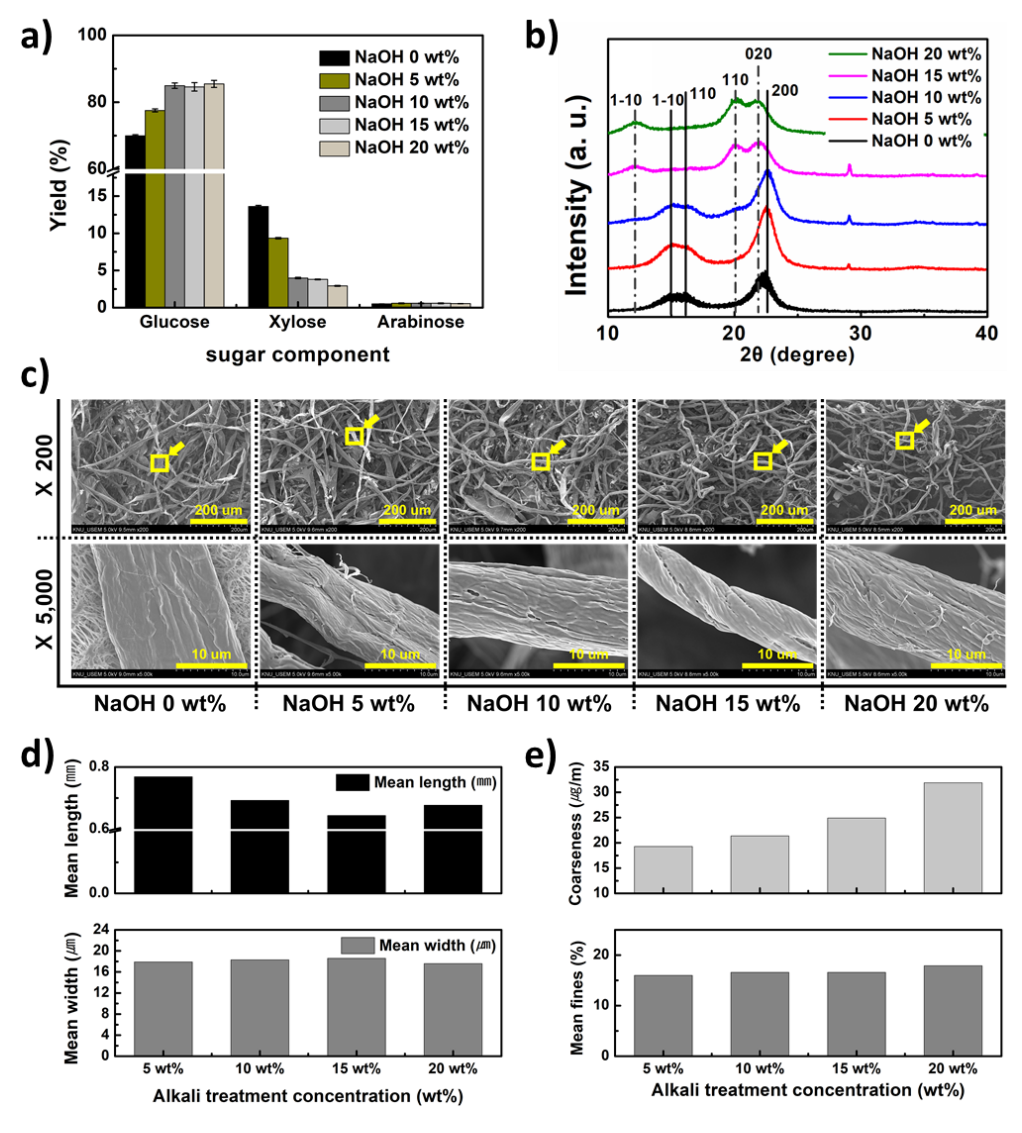


Fig. 1. Changes in (a) sugar composition, (b) XRD patterns, (c) SEM images, and (e, f) fiber analysis of Hw-BKP as a function of alkali pretreatment concentration

The untreated pulp exhibited 70% glucose, 13.6% xylose, and 0.5% arabinose. With increasing NaOH concentration, the glucose content progressively increased, while the xylose content decreased. In particular, pretreatment with NaOH over 10 wt% concentrations resulted in glucose content approaching 85%, accompanied by a sharp reduction in xylose content. This was attributed to the effective removal of hemicellulose even at relatively low alkali concentrations, thereby increasing the relative proportion of cellulose. Arabinose derived from hemicellulose was detected only in trace amounts, showing negligible variation with alkali pretreatment (Carrillo-Varela *et al.* 2022).

Figure 1(b) shows the XRD patterns illustrating the crystalline structural changes of Hw-BKP after alkali pretreatment at concentrations of 0, 5, 10, 15, and 20 wt%. In the untreated and 5 wt% NaOH-treated samples, distinct diffraction peaks corresponding to native cellulose I were observed at $2\theta = 15^{\circ}$ (1-10), 16.5° (110), and 22.3° (200). However, in the 10 wt% NaOH-treated pulp, where hemicellulose was extensively removed, a weak diffraction peak appeared near $2\theta = 20^{\circ}$ (110), which is characteristic of cellulose II with the cellulose I peaks. This indicates that no changes in the cellulose crystal structure occurred at low alkali pretreatment concentrations, whereas partial conversion from cellulose I to cellulose II begins to undergo slight changes at alkali concentrations above 10%.

At NaOH concentrations above 15 wt%, the cellulose I peaks disappeared entirely, and only the characteristic cellulose II peaks at approximately 12° (1-10), 20° (110), and 21.6° (020) were observed, confirming a complete crystalline transformation (French 2014; Ling *et al.* 2017b; Carrillo-Varela *et al.* 2022). This trend is consistent with previous studies, which reported that no crystalline transition occurs below 10 wt% NaOH, whereas cellulose I peak disappeared and the cellulose II peak dominant at NaOH concentrations above 15 wt% (Oh *et al.* 2005; El Oudiani *et al.* 2011a; Yokota *et al.* 2022). These consistent results suggest that the crystal structure conversion occurs robustly under various conditions, from laboratory scale to pilot scale.

This transition can be explained by the structural response of cellulose fibers to alkali exposure. During mercerization, three sequential processes are generally involved: swelling of the fibers, disruption of the crystalline regions, and the formation of a new, thermodynamically stable lattice after the removal of the alkali solution. Liu and Hu wellreported that these sequential transformations govern the overall mercerization behavior of cellulose fibers, with particular emphasis on the balance between fiber swelling and crystalline lattice rearrangement (Liu and Hu 2008). At relatively low NaOH concentrations, the hydroxide ions are fully hydrated and their large hydrated size prevents them from penetrating deeply into the crystalline lattice (Lee et al. 2004). Hence, the alkali reacts primarily with amorphous regions and interfacial components, leading to partial removal of interfibrillar matrix components and a loosening of the interfibrillar structure (Gassan and Bledzki 1999). Conversely, as the NaOH concentration increases, the amount of free water available for hydration decreases, producing smaller, less hydrated hydroxide ions that can penetrate the crystal lattice more easily. This diffusion promotes swelling and relaxation of the cellulose lattice, facilitating the conversion from cellulose I to cellulose II. Upon reaching maximum swelling, extensive ionic penetration and structural rearrangement occur, resulting in the formation of the antiparallel cellulose II structure. Accordingly, in this study, the coexistence of cellulose I and cellulose II was observed at the NaOH concentration of 10 wt%, which was identified as the transition concentration for the structural conversion of cellulose.

Figure 1(c) presents SEM images of pulp fibers treated with various alkali concentrations. SEM analysis showed the structural and surface changes of pulp fibers following NaOH pretreatment. The untreated pulp exhibited thick fibers with minimal inter-fiber entanglement. With increasing NaOH concentration, fiber diameters significantly decreased, and the fibers formed a more densely entangled. The smooth surfaces observed in untreated fibers gradually developed fine wrinkles and partial detachment of the surface layers as the alkali concentration increased. At concentrations above 15 wt%, pronounced helical twisting and extensive fibrillation of the surface microfibrils were evident. These morphological changes are attributed to the removal of matrix components within the cell wall during alkali treatment, fiber swelling induced by water uptake during processing, ion exchange between sodium and hydrogen ions, and subsequent shrinkage during the drying stage (Duchemin 2015; Chen et al. 2017).

Figure 1(d) shows that morphological characteristics (mean fiber length, mean fiber width, coarseness, and fines content) of pulp according to NaOH pretreatment concentration. The mean fiber length decreased with increasing NaOH concentration. This is attributed to the removal of amorphous components such as hemicellulose within the pulp during alkali treatment, which weakened inter-fiber bonding, loosened fiber bundles, and promoted individual fiber separation. At 20 wt%, a slight increase in length was observed, likely due to fiber swelling coupled with chain alignment or re-agglomeration of separated fibers, resulting in some fibers being perceived as longer. The mean fiber width increased slightly with increasing alkali treatment concentration, then decreased again at 20% NaOH. This trend may be explained by fiber swelling and the rearrangement of hydrogen bonds caused by the crystalline transition from cellulose I to cellulose II, which led to a looser fiber structure and thus an apparent increase in width. However, at 20 wt%, the reduction in mean width occurred. This can be due to a combination of factors, including excessive swelling, crystalline transformation, the formation of helical twisting, and fibrillation of surface microfibrils. The fines content showed a slight but consistent increase across treatments. This is consistent with the SEM observations indicating that alkali treatment induced detachment of microfibrils from the fiber surface, generating additional fines. Coarseness increased steadily from 19.3 µg/m to 31.9 µg/m with increasing NaOH concentration. This was likely due to the crystalline transformation and hydrogen bond rearrangement between cellulose chains, leading to enhanced fiber structural densification, aggregation, and increased van der Waals interactions, thereby elevating the relative density (El Oudiani et al. 2011b; Choi et al. 2016; Chen et al. 2017).

Effect of Alkali Pretreatment Concentration on the Properties of Hw-BKP

Mechanical grinding was performed on nanofibrillated pulp pretreated with various concentrations of NaOH, and the results are presented in Fig. 2. Compared with Fig. 1(a), the contents of glucose, xylose, and arabinose in untreated pulp remained nearly constant regardless of the number of grinding cycles. This indicates that mechanical fibrillation alone, without pretreatment, caused negligible degradation of cellulose-derived sugars.

Notable changes were observed in sugar content after mechanical grinding of alkali-treated cellulose fibers. In samples pretreated with below 10 wt% NaOH, the glucose content increased slightly due to the reduction in xylose content resulting from the removal of hemicellulose. In addition, changes in the crystalline structure of pulp were hardly observed. However, contrary to the initial assumption that mechanical grinding would only affect particle size, significant decreases in glucose content were exhibited for pulps pretreated at NaOH concentrations above 15 wt%, where crystalline transformation was

evident. The decrease was 2.42% at 15 wt% and 3.6% at 20 wt%. Moreover, glucose content showed a slight but consistent decrease with increasing grinding cycles across all pretreatment concentrations. As shown in Fig. 1d, after alkaline treatment, microfibrils exhibited little change in thickness but a clear reduction in fiber length. This suggests that alkali pretreatment not only removed hemicellulose but also weakened the amorphous regions within the cellulose main chains, while inducing crystalline transformation (cellulose I-to-II) and reducing crystallinity, making the fibers more susceptible to breakage during mechanical processing (Carrillo-Varela *et al.* 2022). Xylose content decreased with increasing pretreatment concentration but showed no significant change was observed with additional grinding. This is because most hemicellulose was already removed during pretreatment. Arabinose content remained extremely low throughout and was unaffected by any treatment conditions. These results suggest that changes in the sugar composition of pulp are primarily caused by alkaline pretreatment, whereas mechanical treatment alone exerted no substantial effect on compositional changes.

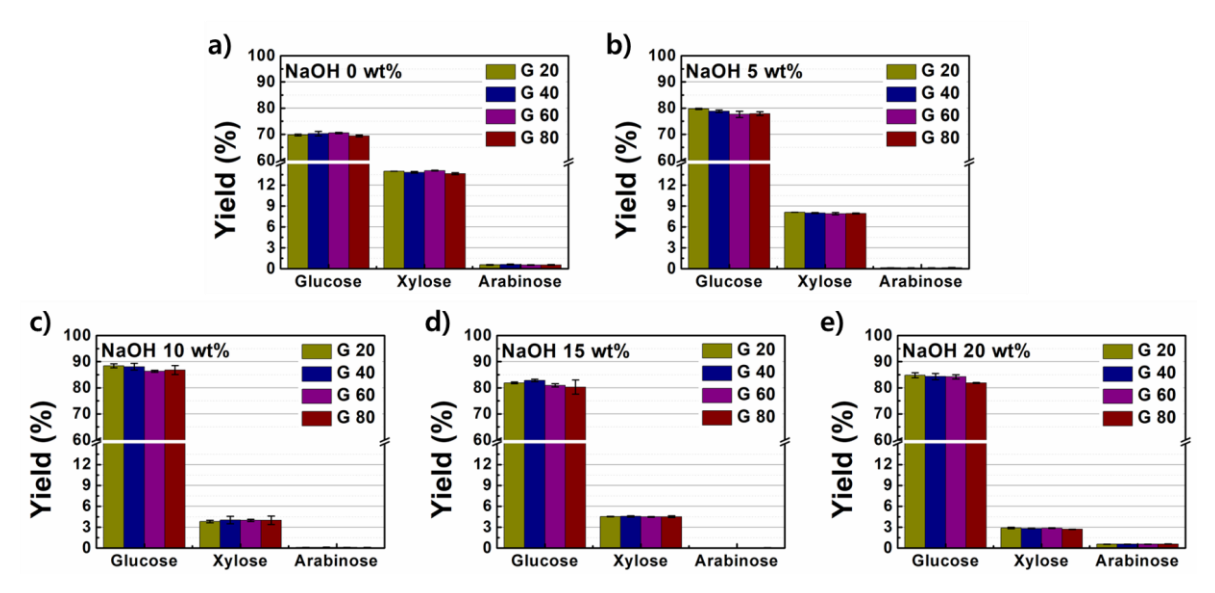


Fig. 2. Sugar composition of Hw-BKP after alkali pretreatment and grinding: (a) untreated, (b) NaOH 5 wt%, (c) NaOH 10 wt%, (d) NaOH 15 wt%, and (e) NaOH 20 wt%

XRD analysis (Fig. 3) was performed to examine the changes in crystalline structure of cellulose pulp according to NaOH pretreatment concentration and the number of grinding passes (G20 to G80). As NaOH increased from 0 to 20 wt%, diffraction patterns progressively shifted from cellulose I to cellulose II. At low concentrations (0 and 5 wt%), typical diffraction peaks of cellulose I were observed at approximately $2\theta = 15^{\circ}$, 16.5° , and 22.3° . In the 10 wt% NaOH-treated pulp, peaks corresponding to cellulose I were accompanied by a new peak near $2\theta = 20^{\circ}$, indicative of partial transformation to cellulose II. At higher concentrations (15–20 wt%), alkali pretreatment induced a complete structural transformation, with cellulose II peaks appearing at approximately $2\theta = 12^{\circ}$, 20° , and 21.6° . However, regardless of the pretreatment concentration, grinding from G20 to G80 did not shift peak positions but gradually reduced their intensities (El Oudiani *et al.* 2011a).

These results indicate that crystalline structure transformation in cellulose is influenced by chemical alkali pretreatment, whereas mechanical fibrillation alone is insufficient to induce such conversion. The observed decrease in XRD peak intensity during grinding is attributed to physical changes such as crystal size reduction and

increased microfibrillation (Supian et al. 2020; Hernández-Becerra et al. 2023; Norfarhana et al. 2024).

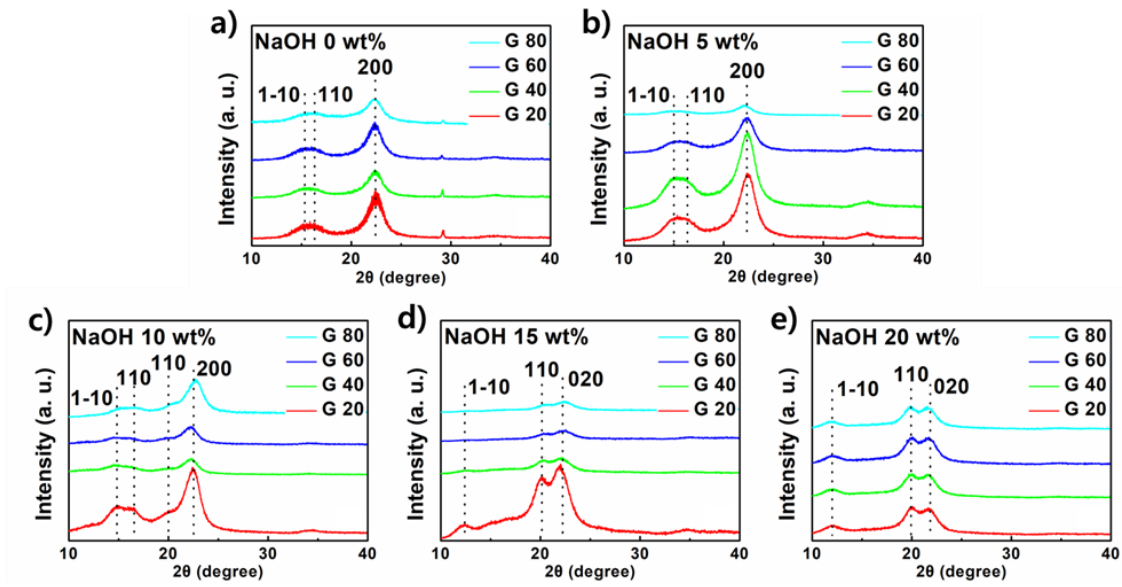


Fig. 3. XRD patterns of Hw-BKP after alkali pretreatment and grinding: (a) untreated, (b) NaOH 5 wt%, (c) NaOH 10 wt%, (d) NaOH 15 wt%, and (e) NaOH 20 wt%

Figure 4 presents optical microscopy images of pulp fibers after alkaline pretreatment (0 to 20 wt% NaOH) and mechanical grinding (20 and 80 passes). At low alkali concentrations, the overall fiber morphology remained almost unchanged. As the alkali concentration increased, however, the fibers became clearly more curled and bent, particularly at concentrations above 10 wt%. These morphological changes are considered to have resulted from the removal of matrix components, including hemicellulose, in the cell wall, as well as from relaxation of the fiber structure caused by swelling and partial dehydration during alkaline treatment. In the 80-pass samples, distinct fibril peeling from the fiber surfaces was observed, and fragmentation and fibrillation progressed further with increasing alkali concentration. This is attributed to the weakening of the fiber structure induced by the crystalline structure transition during NaOH treatment.

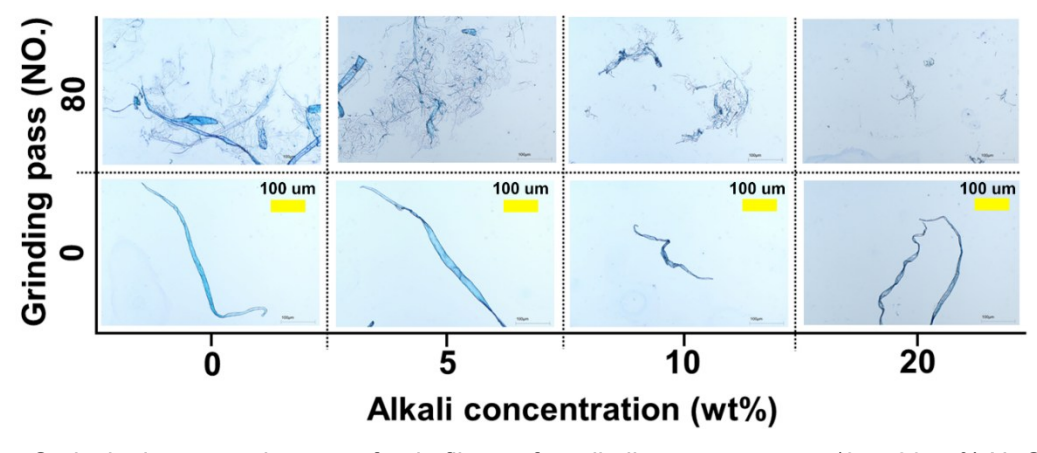


Fig. 4. Optical microscopy images of pulp fibers after alkaline pretreatment (0 to 20 wt% NaOH) and mechanical grinding (0 and 80 passes)

Figures 5 and 6 show the morphological changes of pulp fibers observed by SEM under different NaOH pretreatment concentrations and grinding cycles, at both low (x200) and high (x10k or 30k) magnifications. At low magnification, the number of large microfibers decreased with increasing NaOH concentration and grinding cycles.

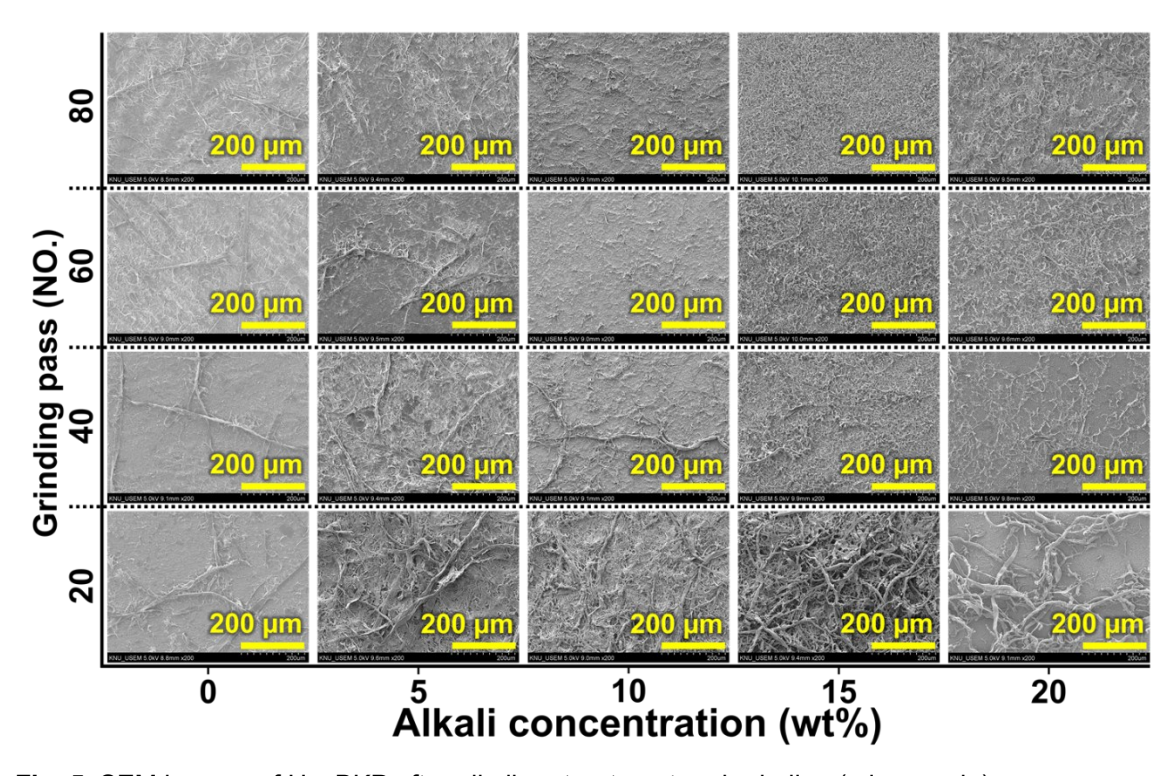


Fig. 5. SEM images of Hw-BKP after alkali pretreatment and grinding (micro scale)

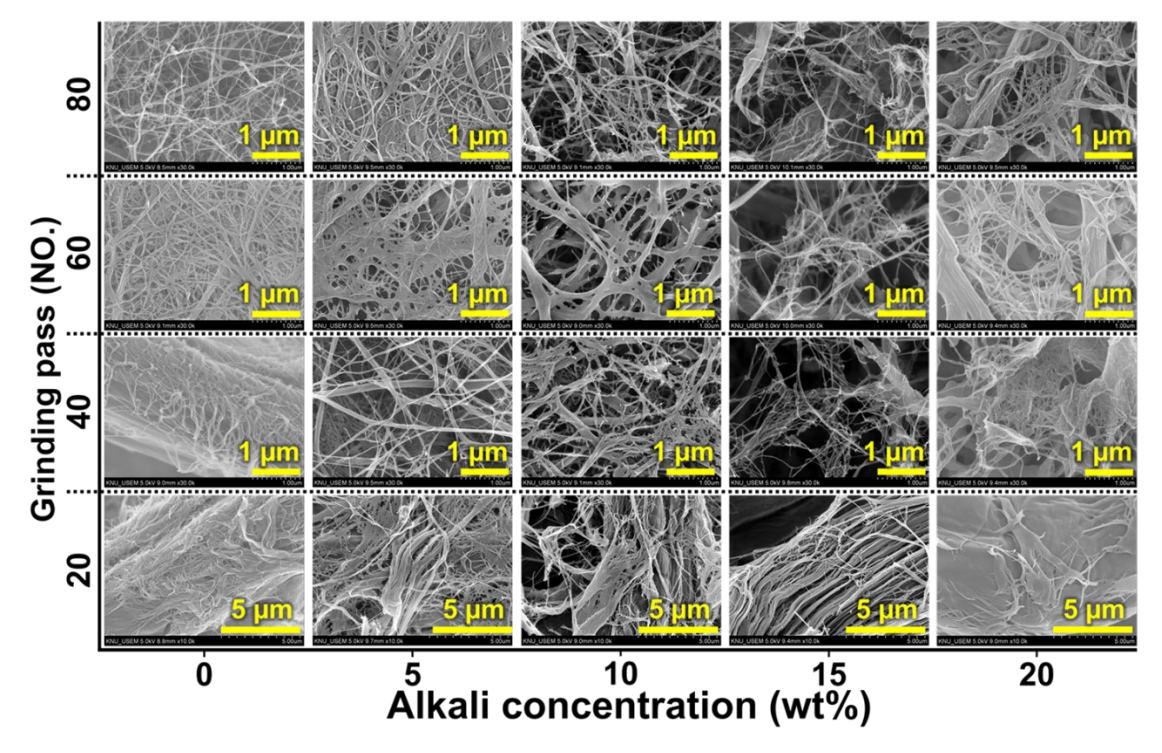


Fig. 6. SEM images of Hw-BKP after alkali pretreatment and grinding (nano scale)

At higher magnifications, nanoscale fibrils were clearly observed on the surfaces of microfibers, and repeated grinding facilitated the fibrillation of fiber bundles into thinner nanofibrils. In particular, up to G20 and G40, higher NaOH concentrations enhanced fibrillation efficiency, resulting in more effective nanofibrillation. However, under higher grinding cycles combined with strong alkali pretreatment (15 to 20 wt%), the fibers exhibited less uniform fibrillation, showing a mixture of fibrils with varying diameters, as well as thicker, aggregated, and twisted structures. This can be attributed to the transformation of cellulose I to cellulose II during high-alkali pretreatment, accompanied by hydrogen bond rearrangement and a reduction in mechanical strength. As a result, shear forces during grinding caused partial fibrils to twist or aggregate rather than forming uniform, straight nanofibers (Wang et al. 2012; Wang et al. 2014; Chen et al. 2017; Hubbe et al. 2017).

Figure 7 shows the variation in fiber width of Hw-BKP under different NaOH pretreatment concentrations and grinding cycles, analyzed from SEM images using ImageJ. The average fiber width was determined from 90 microfibers and 300 nanofibers. The diameters of untreated and alkali-pretreated microfibers (Fig. 7a) were approximately 17.7 to 18.6 µm, and significantly decreased with increasing grinding cycles. The diameter of pulp pretreated with 10 to 20 wt% NaOH exhibited a more reduction compared with untreated and 5 wt% pretreated samples with increasing mechanical treatment times. However, the extent of diameter reduction tended to decrease with increasing alkali concentration. This trend is attributed to the removal of lignin and hemicellulose, together with fiber swelling and weakening during alkali pretreatment, which facilitated microfibrillation under shear forces.

For nanofibers (Fig. 7b), the diameter also decreased as the number of grinding passes increased, but both the mean diameter and the distribution width tended to increase as the NaOH concentration increased. This suggests that, as shown in the SEM results, excessively loosened fiber structures by strong alkali pretreatment underwent entanglement or twisting during mechanical treatment, resulting in relatively thicker fibrils. Moreover, under high-alkali conditions, partial disintegration of cellulose chains followed by re-agglomeration led to the persistence of aggregates during nanofibrillation.

The reproducibility and reliability of the mean width data for both nanofibers and microfibers were assessed using box plots generated with Origin software (OriginLab, USA), as presented in Figs. 7c and 7d. In the box plots, the boxes represent the interquartile range (IQR), which encompasses 50% of the data around the median. The box length indicates the degree of data dispersion, while the horizontal line inside each box corresponds to the median value. When the median line is located near the center of the box, it indicates a uniform distribution of the data, suggesting a high level of consistency and reproducibility in the repeated measurements. A stable data distribution was observed with increasing alkali concentration and the number of grinding cycles. Therefore, alkali pretreatment was identified as a key factor to accelerate fibrillation of pulp, while both pretreatment concentration and grinding cycles determined the degree of fibril defibration and the resulting diameter distribution (Hubbe *et al.* 2017; Wang *et al.* 2012).

Figure 8 presents the UV to Vis transmittance and turbidity results of Hw-BKP suspensions pretreated with alkaline pretreatment and grinder treatment. In the UV-Vis spectra (a–e), transmittance in the range of 200 to 600 nm decreased with increasing grinding cycles under all conditions. In particular, the transmittance of UVA (320 to 400 nm) and UVB (280 to 320 nm) wavelengths decreased markedly, indicating that mechanical treatment enhanced nanofibrillation and thereby increased the concentration of

dispersed nanofibers. Moreover, at higher NaOH pretreatment concentrations, the transmittance decreased more prominently with increasing grinding cycles.

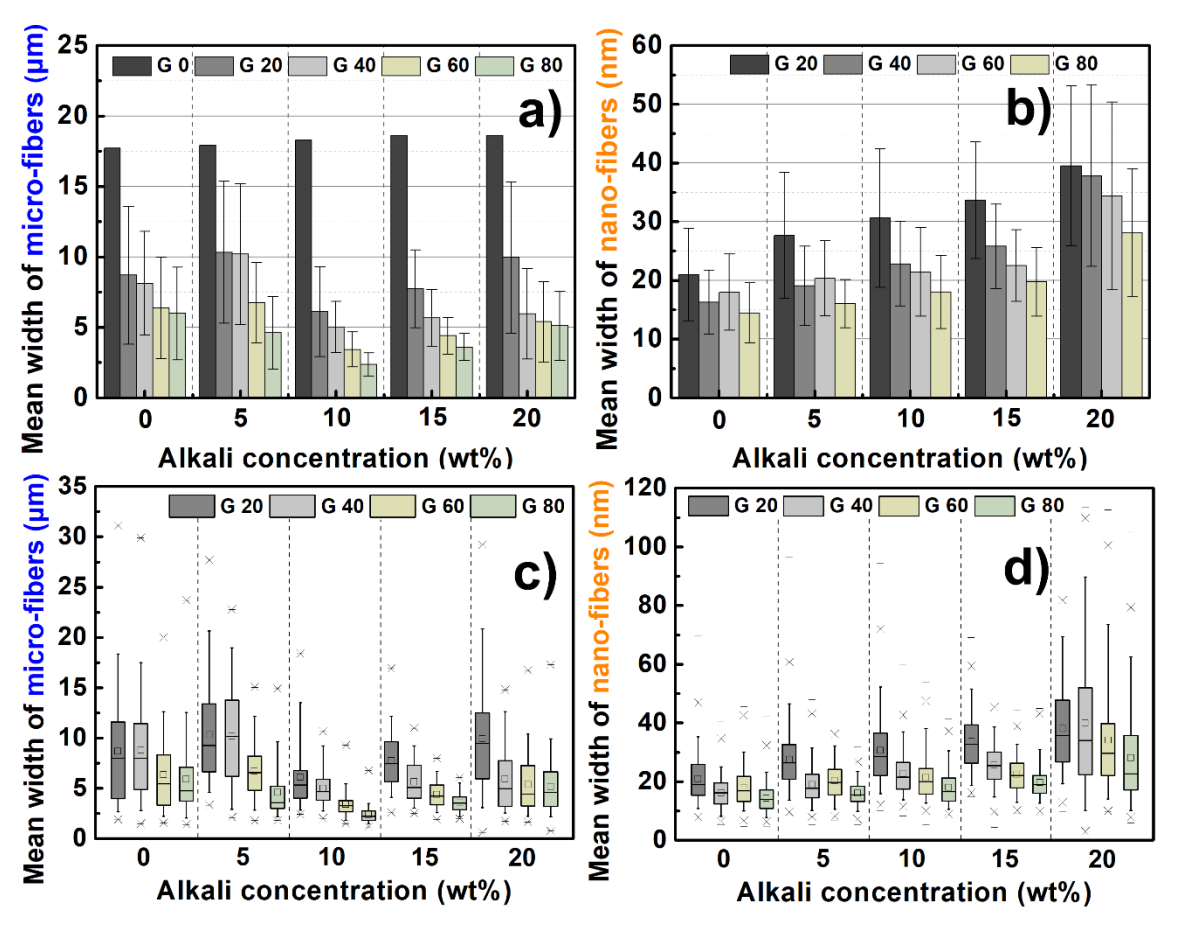


Fig. 7. Fiber width variation of Hw-BKP depending on NaOH pretreatment concentrations and grinding cycles: (a) microfibers and (b) nanofibers from analyzed using ImageJ, (c) & (d) box plot illustrating determined by the micro & nanofiber width variation.

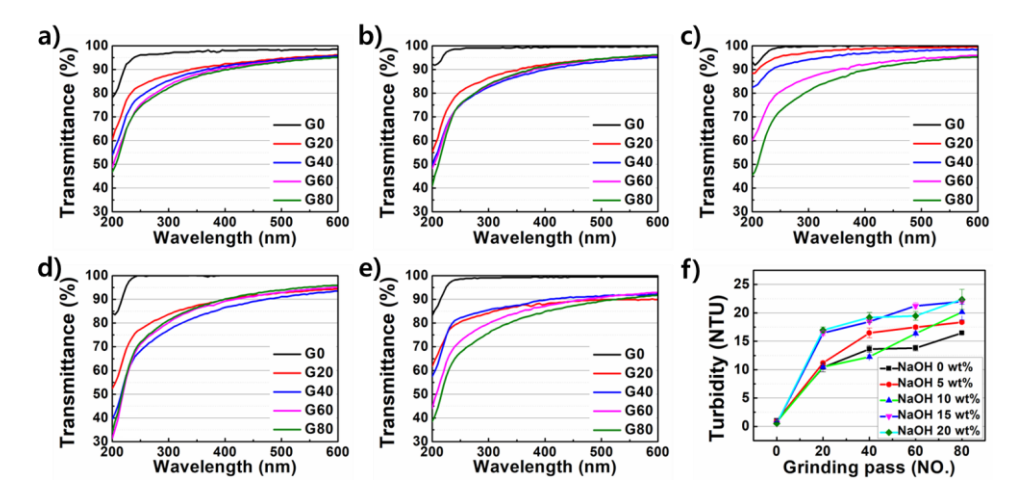


Fig. 8. Optical properties of cellulose nanofiber suspensions prepared from Hw-BKP under different NaOH pretreatment concentrations and grinding cycles: (a) untreated, (b) NaOH 5 wt%, (c) NaOH 10 wt%, (d) NaOH 15 wt%, (e) NaOH 20 wt% UV-Vis transmittance spectra, and (f) turbidity of centrifuged supernatant.

Turbidity analysis (f) revealed that turbidity values increased with both NaOH concentration and grinding passes cycles. This is consistent with the report of Frone et al. (2011), which demonstrated that the progression of nanofibrillation elevates turbidity due to the increased number of dispersed fibrils. In this study, enhanced fibrillation and nanofiber concentration due to alkali pretreatment and the mechanical grinding are considered the primary causes of turbidity increase. Notably, suspensions prepared with high NaOH concentrations (15 to 20 wt%) exhibited higher turbidity values compared to low-concentration pretreatment, suggesting that alkali pretreatment is a key factor for efficient nanofibrillation. Furthermore, Shimizu et al. (2016) reported that an increase in fibril diameter and the formation of aggregate networks in suspension enhance light scattering and consequently increase turbidity. Similarly, Chen et al. (2020) demonstrated that aggregation of cellulose nanocrystals enhances light scattering and consequently increases turbidity in suspension. In this study, SEM observations showed entangled and partially aggregated fibers under high-alkali pretreatment (15 to 20 wt% NaOH), suggesting that both entanglement and aggregation could enhance optical scattering. Therefore, the entanglement and partial aggregation of fibers induced under high-alkali pretreatment can be considered to have contributed to the increase in turbidity.

Based on the sugar content and XRD results shown in Fig. 1(a) and (b), alkali treatment at concentrations below 10 wt% mainly resulted in the reduction of hemicellulose. In contrast, at concentrations above 15 wt%, crystalline structure transformation became more dominant than hemicellulose removal. According to the UV and turbidity analyses, although the nanofibers exhibited an increase in thickness at concentrations above 15 wt%, their content tended to increase qualitatively. Accordingly, in the production of cellulose nanofibers using alkali pretreatment combined with mechanical grinding, not only hemicellulose reduction but also crystalline structural transformation should be considered to improve fibrillation efficiency. Banvillet et al. performed chemical treatment of bleached eucalyptus kraft pulp using 5 to 15% alkali concentrations and investigated the crystallinity of the treated pulp (Banvillet et al. 2021). They reported that the pulp's crystallinity decreased from 40.7% (untreated) to 18.0% (15% alkali-treated). This reduction was attributed to the structural disruption of cellulose by NaOH hydrates occurring during the cellulose II structural transition. Hence, enhancing the fibrillation efficiency can be attributed to the overall structural weakening of cellulose fibers caused by crystalline transformation. Consequently, high-concentration alkali pretreatment above 15 wt% can be an effective approach for nanofibrillation of cellulose fibers by mechanical grinding.

CONCLUSIONS

- 1. Alkali pretreatment effectively removed hemicellulose, increased the relative cellulose content, and induced crystalline transformation from cellulose I to II at 10 wt% NaOH, with complete conversion above 15 wt%. Increasing NaOH concentrations also caused fiber swelling and morphological changes, reducing fiber length and increasing coarseness and fines.
- 2. Mechanical grinding did not affect sugar composition or crystal structure of pulp, but progressive grinding reduced XRD peak intensity and promoted microfibrillation.
- 3. Higher NaOH concentrations improved the fibrillation efficiency by removal of matrix

- components and structural weakening, although excessive pretreatment (15 to 20 wt%) led to entanglement, aggregation, and increased morphological heterogeneity. UV–Vis and turbidity analyses showed consistent trends, confirming that higher NaOH concentrations and longer grinding cycles improved nanofibrillation efficiency.
- 4. The crystalline transition from cellulose I to cellulose II induced by alkaline pretreatment (≥15 wt% NaOH) was closely associated with differences in grinding behavior. Pulp in the cellulose I state (≤10 wt% NaOH) showed limited disintegration due to its higher crystallinity and compact structure, whereas pulp converted to cellulose II (≥15 wt% NaOH) exhibited easier mechanical disintegration, attributed to increased amorphous regions and weakened inter-fiber bonding. Overall, these results indicate that the crystalline allomorph formed by alkaline pretreatment plays a key role in determining the nanofibrillation efficiency of pulp fibers.
- 5. These results demonstrate that, in the fabrication of cellulose nanofibers through alkali pretreatment combined with mechanical grinding, the effect of structural transformation as well as hemicellulose removal plays a decisive role in improving fibrillation efficiency. In particular, alkali pretreatment at concentrations above 15 wt% provides a highly effective approach to enhancing the production efficiency of cellulose nanofibers.

ACKNOWLEDGMENTS

This study was supported by the National Institute of Forest Science (grant number: FP0701-2021-02) and Korea Forest Service (grant number: 2021354A00-2023-AC03-1).

REFERENCES CITED

- Banvillet, G., Depres, G., Belgacem, N., and Bras, J. (2021). "Alkaline treatment combined with enzymatic hydrolysis for efficient cellulose nanofibrils production," *Carbohydrate Polymers* 255, article 117383. https://doi.org/10.1016/j.carbpol.2020.117383
- Barhoum, A., Pal, K., Rahier, H., Uludag, H., Kim, I. S., and Bechelany, M. (2019). "Nanofibers as new-generation materials: From spinning and nano-spinning fabrication techniques to emerging applications," *Appl. Mater. Today* 17, 1-35. https://doi.org/10.1016/j.apmt.2019.06.015
- Cao, L., Zhu, J., Deng, B., Zeng, F., Wang, S., Ma, Y., Qin, C., and Yao, S. (2022). "Efficient swelling and mercerization of bagasse fiber by freeze-thaw-assisted alkali treatment," *Front. Energy Res.* 10, article 851543. https://doi.org/10.3389/fenrg.2022.851543
- Carrillo-Varela, I., Vidal, C., Vidaurre, S., Parra, C., Machuca, Á., Briones, R., and Mendonça, R. T. (2022). "Alkalization of kraft pulps from pine and eucalyptus and its effect on enzymatic saccharification and viscosity control of cellulose," *Polymers* 14(15), 3127-3148. https://doi.org/10.3390/polym14153127
- Carter, N., Grant, I., Dewey, M., Bourque, M., and Neivandt, D. J. (2021). "Production and characterization of cellulose nanofiber slurries and sheets for biomedical applications," *Front. Nanotechnol.* 3, article 729743.

- https://doi.org/10.3389/fnano.2021.729743
- Chen, H., Yu, Y., Zhong, T., Wu, Y., Li, Y., Wu, Z., and Fei, B. (2017). "Effect of alkali treatment on microstructure and mechanical properties of individual bamboo fibers," *Cellulose* 24(1), 333-347. https://doi.org/10.1007/s10570-016-1144-7
- Chen, M., Parot, J., Mukherjee, A., Couillard, M., Zou, S., Hackley, V. A., and Johnston, L. J. (2020). "Characterization of size and aggregation for cellulose nanocrystal dispersions separated by asymmetrical-flow field-flow fractionation," *Cellulose* 27(4), 2015-2028. https://doi.org/10.1007/s10570-019-02909-9
- Choi, K. H., Kim, A. R., and Cho, B. U. (2016). "Effects of alkali swelling and beating treatments on properties of kraft pulp fibers," *BioResources* 11(2), 3769-3782. https://doi.org/10.15376/biores.11.2.3769-3782
- Dinand, E., Vignon, M., Chanzy, H., and Heux, L. (2002). "Mercerization of primary wall cellulose and its implication for the conversion of cellulose I→cellulose II," *Cellulose* 9, 7-18.
- Djafari Petroudy, S. R., Chabot, B., Loranger, E., Naebe, M., Shojaeiarani, J., Gharehkhani, S., Ahvazi, B., Hu, J., and Thomas, S. (2021). "Recent advances in cellulose nanofibers preparation through energy-efficient approaches: A review," *Energies* 14(20), 6792-6822. https://doi.org/10.3390/en14206792
- Duchemin, B. J. C. (2015). "Mercerisation of cellulose in aqueous NaOH at low concentrations," *Green Chem.* 17, 3941-3947. https://doi.org/10.1039/C5GC00597H
- El Oudiani, A., Chaabouni, Y., Msahli, S., and Sakli, F. (2011). "Crystal transition from cellulose I to cellulose II in NaOH treated *Agave americana* L. fibre," *Carbohydr. Polym.* 86(3), 1221-1229. https://doi.org/10.1016/j.carbpol.2011.06.037
- French, A. D. (2014). "Idealized powder diffraction patterns for cellulose polymorphs," *Cellulose* 21(2), 885-896. https://doi.org/10.1007/s10570-013-0030-4
- Frone, A. N., Panaitescu, D. M., Donescu, D., Spataru, C. I., Radovici, C., Trusca, R., and Somoghi, R. (2011). "Preparation and characterization of PVA composites with cellulose nanofibers obtained by ultrasonication," *BioResources* 6(1), 487-512. https://doi.org/10.15376/biores.6.1.487-512
- Ganesan, A., and Rengarajan, J. (2022). "A review on fabrication methods of nanofibers and a special focus on application of cellulose nanofibers," *Carbohydr. Polym. Technol. Appl.* 4, 100262-100275. https://doi.org/10.1016/j.carpta.2022.100262
- Gassan, J., and Bledzki, A. K. (1999). "Possibilities for improving the mechanical properties of jute/epoxy composites by alkali treatment of fibres," *Composites Science and Technology* 59(9), 1303-1309. https://doi.org/10.1016/S0266-3538(98)00169-9
- Hajikhani, M., and Lin, M. (2022). "A review on designing nanofibers with high porous and rough surface via electrospinning technology for rapid detection of food quality and safety attributes," *Trends Food Sci. Technol.* 128, 118-128. https://doi.org/10.1016/j.tifs.2022.08.003
- Hernández-Becerra, E., Osorio, M., Marín, D., Gañán, P., Pereira, M., Builes, D., and Castro, C. (2023). "Isolation of cellulose microfibers and nanofibers by mechanical fibrillation in a water-free solvent," *Cellulose* 30(8), 4905-4923. https://doi.org/10.1007/s10570-023-05110-3
- Hiwrale, A., Bharati, S., Pingale, P., and Rajput, A. (2023). "Nanofibers: A current era in drug delivery system," *Heliyon* 9(9), article e18917. https://doi.org/10.1016/j.heliyon.2023.e18917
- Hubbe, M. A., Tayeb, P., Joyce, M., Tyagi, P., Kehoe, M., Dimic-Misic, K., and Pal, L.

- (2017). "Rheology of nanocellulose-rich aqueous suspensions: A review," *BioResources* 12(4), 9556-9661. https://doi.org/10.15376/biores.12.4.9556-9661
- Jonoobi, M., Oladi, R., Davoudpour, Y., Oksman, K., Dufresne, A., Hamzeh, Y., and Davoodi, R. (2015). "Different preparation methods and properties of nanostructured cellulose from various natural resources and residues: A review," *Cellulose* 22(2), 935-969. https://doi.org/10.1007/s10570-015-0551-0
- Jose, S. A., Cowan, N., Davidson, M., Godina, G., Smith, I., Xin, J., and Menezes, P. L. (2025). "A comprehensive review on cellulose nanofibers, nanomaterials, and composites: Manufacturing, properties, and applications," *Nanomaterials* 15(5), 356-388. https://doi.org/10.3390/nano15050356
- Kassie, B. B., Daget, T. M., and Tassew, D. F. (2024). "Synthesis, functionalization, and commercial application of cellulose-based nanomaterials," *Int. J. Biol. Macromol.* 278(4), 134990-135018. https://doi.org/10.1016/j.ijbiomac.2024.134990
- Ke, Y., Huang, L., Song, Y., Liu, Z., Liang, L., Wang, L., and Wang, T. (2022). "Preparation and pharmacological effects of minor ginsenoside nanoparticles: A review," *Front. Pharmacol.* 13, 974274. https://doi.org/10.3389/fphar.2022.974274
- Kobayashi, K., Kimura, S., Kim, U.-J., Tokuyasu, K., and Wada, M. (2012). "Enzymatic hydrolysis of cellulose hydrates," *Cellulose* 19, 967-974. https://doi.org/10.1007/s10570-012-9696-2
- Kuo, C.-H., and Lee, C.-K. (2009). "Enhancement of enzymatic saccharification of cellulose by cellulose dissolution pretreatments," *Carbohydrate Polymers* 77(1), 41-46. https://doi.org/10.1016/j.carbpol.2008.12.003
- Lee, M. H., Park, H. S., Yoon, K. J., and Hauser, P. J. (2004). "Enhancing the durability of linen-like properties of low temperature mercerized cotton," *Text. Res. J.* 74(2), 146-154. https://doi.org/10.1177/004051750407400211
- Ling, Z., Chen, S., Zhang, X., and Xu, F. (2017a). "Exploring crystalline-structural variations of cellulose during alkaline pretreatment for enhanced enzymatic hydrolysis," *Bioresource Technology* 224, 611-617. https://doi.org/10.1016/j.biortech.2016.10.064
- Ling, Z., Chen, S., Zhang, X., Takabe, K., and Xu, F. (2017b). "Unraveling variations of crystalline cellulose induced by ionic liquid and their effects on enzymatic hydrolysis," *Sci. Rep.* 7(1), article 10230. https://doi.org/10.1038/s41598-017-09885-9
- Liu, Y., and Hu, H. (2008). "X-ray diffraction study of bamboo fibers treated with NaOH," *Fibers and Polymers* 9, 735-839.
- Meyabadi, T. F., Dadashian, F., Sadeghi, G. M. M., and Zanjani Asl, H. E. (2014). "Spherical cellulose nanoparticles preparation from waste cotton using a green method," *Powder Technol.* 261, 232-240. https://doi.org/10.1016/j.powtec.2014.04.039
- Michelin, M., Gomes, D. G., Romaní, A., Polizeli, M. L. T. M., and Teixeira, J. A. (2020). "Nanocellulose production: Exploring the enzymatic route and residues of pulp and paper industry," *Molecules* 25(15), 3411-3446. https://doi.org/10.3390/molecules25153411
- Nechyporchuk, O., Belgacem, M. N., and Bras, J. (2016). "Production of cellulose nanofibrils: A review of recent advances," *Ind. Crops Prod.* 93, 2-25. https://doi.org/10.1016/j.indcrop.2016.02.016
- Norfarhana, A. S., Ilyas, R. A., Ngadi, N., and Othman, M. H. D. (2024). "Innovative ionic liquid pretreatment followed by wet disk milling treatment provides enhanced

- properties of sugar palm nano-fibrillated cellulose," *Heliyon* 10(6), article e27715. https://doi.org/10.1016/j.heliyon.2024.e27715
- Oh, S. Y., Yoo, D. I., Shin, Y., Kim, H. C., Kim, H. Y., Chung, Y. S., Park, W. H., and Youk, J. H. (2005). "Crystalline structure analysis of cellulose treated with sodium hydroxide and carbon dioxide by means of X-ray diffraction and FTIR spectroscopy," *Carbohydr. Res.* 340(15), 2376-2391. https://doi.org/10.1016/j.carres.2005.08.007
- Pradhan, D., Jaiswal, A. K., and Jaiswal, S. (2022). "Emerging technologies for the production of nanocellulose from lignocellulosic biomass," *Carbohydr. Polym.* 285, 119258-119277. https://doi.org/10.1016/j.carbpol.2022.119258
- Shimizu, M., Saito, T., Nishiyama, Y., Iwamoto, S., Yano, H., Isogai, A., and Endo, T. (2016). "Fast and robust nanocellulose width estimation using turbidimetry," *Macromol. Rapid Commun.* 37(19), 1581-1586. https://doi.org/10.1002/marc.201600357
- Spence, K. L., Venditti, R. A., Rojas, O. J., Habibi, Y., and Pawlak, J. J. (2011). "A comparative study of energy consumption and physical properties of microfibrillated cellulose produced by different processing methods," *Cellulose* 18, 1097-1111. https://doi.org/10.1007/s10570-011-9533-z
- SriBala, G., Chennuru, R., Mahapatra, S., and Vinu, R. (2016). "Effect of alkaline ultrasonic pretreatment on crystalline morphology and enzymatic hydrolysis of cellulose," *Cellulose* 23, 1725-1740. https://doi.org/10.1007/s10570-016-0893-2
- Supian, M. A. F., Amin, K. N. M., Jamari, S. S., and Mohamad, S. (2020). "Production of cellulose nanofiber (CNF) from empty fruit bunch (EFB) *via* mechanical method," *J. Environ. Chem. Eng.* 8(1), article 103024. https://doi.org/10.1016/j.jece.2019.103024
- Wang, H., Li, D., Yano, H., and Abe, K. (2014). "Preparation of tough cellulose II nanofibers with high thermal stability from wood," *Cellulose* 21(3), 1505-1515. https://doi.org/10.1007/s10570-014-0184-8
- Wang, Q. Q., Zhu, J. Y., Gleisner, R., Kuster, T. A., Baxa, U., and McNeil, S. E. (2012). "Morphological development of cellulose fibrils of a bleached eucalyptus pulp by mechanical fibrillation," *Cellulose* 19(5), 1631-1643. https://doi.org/10.1007/s10570-012-9745-x
- Yao, C., Li, F., Chen, T., and Tang, Y. (2023). "Green preparation of cellulose nanofibers via high-pressure homogenization and their film-forming properties," *Ind. Crops Prod.* 206, 117575-117586. https://doi.org/10.1016/j.indcrop.2023.117575
- Yokota, S., Nishimoto, A., and Kondo, T. (2022). "Alkali-activation of cellulose nanofibrils to facilitate surface chemical modification under aqueous conditions," *J. Wood Sci.* 68, 14. https://doi.org/10.1186/s10086-022-02022-9
- Yue, Y., Han, G., and Wu, Q. (2013). "Transitional properties of cotton fibers from cellulose I to cellulose II structure," *BioResources* 8(4), 6460-6471. https://doi.org/10.15376/biores.8.4.6460-6471

Article submitted: August 21, 2025; Peer review completed: October 25, 2025; Revised version received and accepted: November 2, 2025; Published: November 17, 2025. DOI: 10.15376/biores.21.1.288-304